

Photochemical & Photobiological Sciences

Accepted Manuscript



This is an *Accepted Manuscript*, which has been through the Royal Society of Chemistry peer review process and has been accepted for publication.

Accepted Manuscripts are published online shortly after acceptance, before technical editing, formatting and proof reading. Using this free service, authors can make their results available to the community, in citable form, before we publish the edited article. We will replace this *Accepted Manuscript* with the edited and formatted *Advance Article* as soon as it is available.

You can find more information about *Accepted Manuscripts* in the [Information for Authors](#).

Please note that technical editing may introduce minor changes to the text and/or graphics, which may alter content. The journal's standard [Terms & Conditions](#) and the [Ethical guidelines](#) still apply. In no event shall the Royal Society of Chemistry be held responsible for any errors or omissions in this *Accepted Manuscript* or any consequences arising from the use of any information it contains.



Photochemical & Photobiological Science

Paper

Role of Cr(III) deposition during the photocatalytic transformation of hexavalent chromium and citric acid over commercial TiO₂ samples

V. N. Montesinos,^{ab} C. Salou^c, J. M. Meichtry^{ab}, C. Colbeau-Justin^c and M. I. Litter^{*abd}

Received 00th January 20xx,
Accepted 00th January 20xx

DOI: 10.1039/x0xx00000x

www.rsc.org/

Removal of Cr(VI) and citric acid (Cit) by heterogeneous photocatalytic Cr(VI) transformation under UV light over two commercial TiO₂ samples (1 g L⁻¹), Evonik P25 and Hombikat UV100, was studied at pH 2 and Cr(VI) concentrations between 0.2 and 3 mM, with a fixed [Cit]₀/[Cr(VI)]₀ molar ratio (MR) of 2.5. In both cases, up to complete Cr(VI) removal, the temporal profiles of Cr(VI) and Cit were well adjusted to a pseudo-first order rate law with the same rate constant, evidencing that Cr(VI) removal controls the kinetics of the system. Once Cr(VI) is fully removed, Cit degradation continues with a Langmuir-Hinshelwood behaviour. In all cases, the rate constants decreased with increasing [Cr(VI)]₀, and time resolved microwave conductivity (TRMC) measurements revealed that it was due to an increasing retention of Cr(III) on the surface of the photocatalysts, which reduces the lifetime of the electrons. Both kinetic experiments and TRMC measurements confirm that UV100 is not only more efficient than P25 for Cr(VI) and Cit removal, but it is also less influenced by the poisoning of the surface, consistently with its larger specific area. The use of Cit as the sacrificial agent improves the rate and efficiency of the photocatalytic Cr(VI) removal, and also the stability of the photocatalyst by preventing Cr(III) deposition, due to the formation of soluble Cr(III)-complexes, envisaged as a general result of the presence of oligocarboxylic acids in the photocatalytic Cr(VI) system.

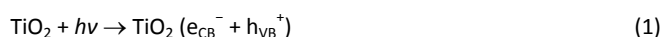
Introduction

Hexavalent chromium is a toxic (carcinogenic) water pollutant, which can be found naturally^{1,2} or be present in waters coming from anthropic sources due to multiple industrial applications (e.g. metallurgy, paintings, textile industry, wood, etc.).³ Its presence in water bodies causes high environmental and social impact,⁴ and recently, several incidents related with pollution of water by Cr(VI) have been reported.^{5,6} As Cr(III) is far less toxic and mobile, reduction is a very convenient treatment for Cr(VI) containing wastewaters.

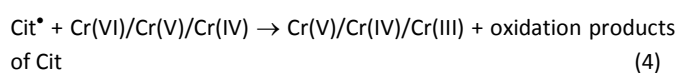
Cr(VI) removal by heterogeneous photocatalysis (HP) has been extensively studied, and a plethora of studies has been carried out on this system, especially by our group; reviews on this subject have been published,⁷⁻¹¹ and the specific references can be consulted there. It is very well established that the addition of a sacrificial electron donor has a profound effect on the enhancement of the Cr(VI) photocatalytic transformation,

and EDTA, oxalic acid and citric acid (Cit) have been tested, among others. Previous works¹²⁻¹⁵ compared different organic donors, and it was observed that Cit was one of the best agents to improve the reaction. Cit is an organic model compound of low toxicity normally present in waters and soils, and coexists with chromium in some natural systems.² Besides, it has the ability to complex and to stabilize Cr(V), a proven intermediate in the HP reduction of Cr(VI) to Cr(III) over TiO₂. The photocatalytic Cr(VI)/Cit system has been also analysed previously by us,^{16,17} and others (e.g. Refs.^{18,19}).

The mechanism of TiO₂ photocatalytic reduction of Cr(VI) has been thoroughly studied (see e.g. Refs.^{8-11,14-21}). It is accepted that HP reduction proceeds through three successive one electron reactions of Cr(VI) with electrons of the conduction band (e_{CB}⁻) generated after irradiation of the semiconductor.



As an electron donor, Cit captures the h_{VB}⁺, decreasing the recombination ratio of e⁻/h⁺ pairs, thereby enhancing Cr(VI) removal, with the additional advantage of the generation of reducing radicals, which contribute also to the Cr(VI) decay:



^a Gerencia Química, Centro Atómico Constituyentes, CNEA, Av. Gral. Paz 1499, 1650 San Martín, Prov. de Buenos Aires, Argentina.

^b CONICET, Rivadavia 1917, Buenos Aires, Argentina

^c Laboratoire de Chimie Physique, CNRS UMR 8000, Université Paris-Sud 11, Bâtiment 349, 91405 Orsay Cedex, France.

^d Instituto de Investigación e Ingeniería Ambiental, Universidad de General San Martín, Campus Miguelete, Av. 25 de Mayo y Francia, 1650 San Martín, Prov. de Buenos Aires, Argentina

† Electronic Supplementary Information (ESI) available: Cr(VI) and Cit adsorption on P25 and UV100, homogeneous photochemical removal of Cr(VI) in the presence of Cit, photocatalytic kinetic parameters, TRMC fundamentals and results. See DOI: 10.1039/x0xx00000x

However, several aspects of the Cr(VI)-Cit system still merit discussion, such as the effect of the Cr(VI) concentration, the nature of the photocatalyst on the reaction rate and the role of Cr(III) deposited on the surface of the photocatalyst. These variables are analysed in the present paper using the commercial TiO₂ samples Evonik P25 and Hombikat UV100, the most widely used materials in the photocatalytic field (see e.g. Refs.^{20,21}). In addition, TRMC runs were done with the purpose of determining the influence of surface retained Cr(III) on the photocatalytic performance.

Experimental

Chemicals

TiO₂ Degussa P25 and Hombikat UV100 were provided by Degussa AG Germany (now Evonik) and Sachtleben, respectively, and used as received. Phase composition, particle size and specific surface area (SSA) of each photocatalyst were measured and can be found in a previous study of our group.²⁰ Cr(VI) (K₂Cr₂O₇, 99.9% Merck), Cit (C₆H₈O₇·H₂O, 99% Riedel de Hën), 3-oxoglutaric acid (OGA, 1,3-acetonedicarboxylic acid, Sigma-Aldrich), acetoacetic acid (AAA, from the lithium salt, Sigma-Aldrich), and all other chemicals were reagent grade. HClO₄ (70%) was Merck. In all experiments, Milli-Q water was used (resistivity = 18 MΩ·cm).

Irradiation Procedure

Irradiation experiments were performed using a batch recirculating reactor consisting in a glass jacketed reservoir, a peristaltic pump (Apema BS6) and a photoreactor equipped with a Toshiba black light lamp (310 < λ/nm < 410, λ_{max} = 351 nm) centred in a glass tube, with the suspension circulating in the space between the lamp and the tube. A TiO₂ suspension (350 mL, 1 g L⁻¹) containing Cr(VI) at various concentrations (0.2 < [Cr(VI)]₀/mM ≤ 3, the typical concentration range found in industrial wastewaters)³ and Cit was adjusted to pH 2 with diluted HClO₄. In all experiments, the [Cit]₀/[Cr(VI)]₀ molar ratio (MR) was 2.5 because this MR has shown the higher efficiency for Cr(VI) HP reduction.¹⁷ The suspension was continuously recirculated (1.5 L min⁻¹) using the peristaltic pump. Air was bubbled at 1 L min⁻¹ into the reservoir, from where samples were taken for analysis. The irradiated volume in the photoreactor was 90 mL; the incident photon flux per unit volume ($q_{n,p}^0/V$) was 15.2 μeinstein s⁻¹ L⁻¹, as determined by ferrioxalate actinometry in the same conditions as those of the HP experiments. Prior to irradiation, suspensions were recirculated in the dark for 30 min to ensure substrate-surface equilibration. All the experiments were carried out at 25 °C controlled by a thermocirculator (PolyScience).

Analysis of samples

Cr(VI) concentration was followed by the spectrophotometric diphenylcarbazide method,²² measuring at 540 nm. Evolution of Cit and organic compounds formed during the photocatalytic runs were followed by HPLC, modifying the technique from Ref.²³ Briefly, an Alltech301 HPLC pump with a

UV/VIS Thermo Separation Products UV 100 detector (detection at 210 nm for all compounds except acetone, measured at 263 nm) and a Konikrom Chromatography Data System V.5.2 were used. A C-18 Restek Ultra Aqueous, 250 × 4.6 mm column was employed; H₃PO₄ buffer (pH 2.1), at 1 mL min⁻¹ flow rate, was the eluent. Periodical samples (0.5-2 mL) were taken, filtered through 0.2 μm cellulose acetate filters (Sartorius) and diluted to 10 mL with the same eluent for the analysis.

TRMC measurements

The solids from selected photocatalytic experiments obtained after complete Cr(VI) removal were separated by filtration, dried for 24 h at 50 °C and analysed by TRMC. The samples were put on a glass plate (Corning 7059) and placed on the extremity of a waveguide cavity (WR28). Microwaves were generated by a GUNN diode (K_α band, 30 GHz). The excitation was performed at 355 nm using an OPO laser (NT342B, EKSPILA). Full-width at half-maximum (FWHM) was 8 ns; repetition frequency of the pulses was 10 Hz. The light energy density received by the sample from each pulse was around 1.4 mJ cm⁻². Reflected microwaves from the excited samples were detected by a band detector (Agilent R422C), which turns microwave signal into electric signal, and then amplified (200 MHz, 60 dB). The TRMC signal was finally represented by means of a digitizer (LeCroyLT374).

Total Cr over TiO₂

Total Cr content over TiO₂ (Cr@TiO₂) was measured by total reflection X-ray fluorescence (TXRF) in the solid samples used for TRMC analyses. The solids were resuspended in water and mixed with a Ga(II) standard solution to reach 1 g L⁻¹ of the solid and 10 mg L⁻¹ of Ga(II). A drop of 10 μL of each suspension was carefully seeded and dried over an acrylic disc and then inserted in a S2 Picofox TXRF spectrometer. The amount of Cr in the TiO₂ samples was expressed as equivalent concentration (mmol of Cr/g of TiO₂).

Diffuse absorbance measurements

Absorption spectra of the solids used for TRMC analysis were taken with a Cary 5000 UV-Vis-NIR spectrometer (Agilent) with a diffuse reflectance accessory in the range 200-800 nm. The baseline was recorded using a poly(tetrafluoroethylene) reference.

Results and discussion

Photocatalytic removal of Cr(VI) and Cit

Before irradiation, part of the Cit and Cr(VI) initially present in the system was adsorbed on the surface after 30 min in the dark, with no further changes after 120 min (Fig. S1, electronic supporting information, ESI). After the adsorption equilibrium was reached, irradiation of the system under UV light led to photocatalytic Cr(VI) reduction and Cit oxidation, with formation of OGA and AAA.¹⁷ As previously indicated,²³ AAA is formed exclusively from the thermal degradation of OGA; thus,

the sum of OGA and AAA was taken as OGA to reflect only the changes produced by irradiation. Fig. 1 shows the time evolution of Cr(VI), Cit and OGA concentrations for the photocatalytic reaction of 0.4 mM Cr(VI) in the presence of Cit (MR = 2.5) over P25 and UV100 (1 g L⁻¹) at pH 2 and under air bubbling. Once all the Cr(VI) present in the system was removed, Cit degradation continues using O₂ as electron acceptor. Changes in pH were negligible during the irradiation time.

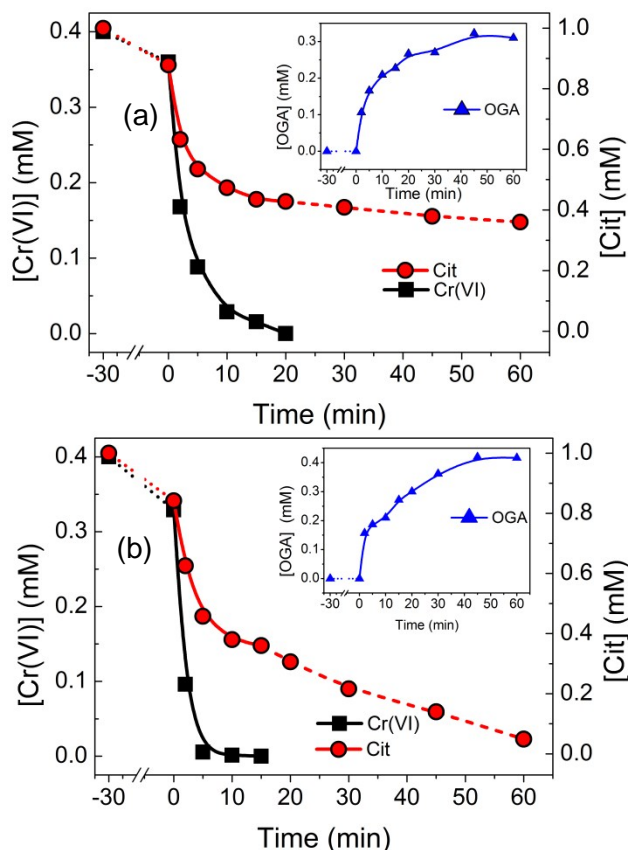


Fig. 1. Temporal profiles of [Cr(VI)] and [Cit] during removal of Cr(VI) by HP in the presence of (a) P25 and (b) UV100. Conditions: [Cr(VI)]₀ = 0.4 mM, [Cit]₀ = 2.5 mM, [TiO₂] = 1 g L⁻¹, P25, UV irradiation (310 < λ/nm < 410, λ_{max} = 351 nm; q_{0,p}/V = 15.2 μeinstein s⁻¹ L⁻¹). The dotted lines represent changes in the dark before irradiation. The solid lines are the fitting of the experimental points to a pseudo-first order rate law. The dashed lines represent Cit degradation after Cr(VI) total removal fitted to a LH rate law. Inset: temporal profiles for OGA evolution. The blue solid lines are only for a better visualization of points and do not correspond to any fitting model.

Profiles of other [Cr(VI)]₀ were similar. The profiles obtained when using UV100 present the same general behaviour as those obtained with P25, but a higher rate is observed for the evolution of the three involved species, pointing out a higher activity. After Cr(VI) consumption, UV100 presented a higher efficiency than P25 for Cit degradation, but the trend was also similar.

Cr(VI) photocatalytic temporal decay was satisfactorily fitted to a pseudo-first order rate for all Cr(VI) concentrations and both photocatalysts ($R^2 \geq 0.98$, Tables S1 and S2). As can be seen in Fig. 1, Cr(VI) and Cit temporal profiles run in parallel until Cr(VI) is completely removed, suggesting that Cr(VI) removal controls the reaction rate. This was proved by the fitting of the temporal profile of Cit concentration also to a pseudo-first

order rate law ($R^2 \geq 0.94$) using the same pseudo-first order constant (k_1) obtained for Cr(VI) (Tables S1 and S2).

After all Cr(VI) is removed from the system, Cit degradation continues and the experimental points could be very well fitted to a LH rate law equation (see ESI, eq. (S1)). The fitting parameters are shown in Tables S3 and S4, and the adjustment is represented by the dashed lines in Fig. 1.

The fitting of the experimental points of OGA evolution according to Ref.²³ was not included as no additional conclusion could be extracted from this analysis.

According to previous results at the same pH and concentration range used in this work, Cit oxidation by HP with O₂ as electron acceptor leads to the formation of OGA with 100% selectivity following a Langmuir-Hinshelwood (LH) rate law.²⁴ However, in the presence of Cr(VI), the selectivity towards OGA formation is considerably lower as can be seen in Fig. S3 (see ESI, eq. (S2)). As OGA was detected as the only degradation product of Cit in the present photocatalytic experiments, and given that OGA was reported to be negligibly adsorbed on the surface of TiO₂,²³ the lower OGA selectivity could be explained by the formation of Cr(III) complexes with Cit, OGA or other undetected organic by-products. Evidence of Cr(III)-Cit and Cr(III)-OGA complexes in a similar system were thoroughly analysed by Meichtry et al. by UV-Vis spectrometry.^{16,17}

Despite the good fitting obtained for the experimental points, both k_1 , the pseudo-first order rate constant for Cr(VI) and Cit concerted removal, and $k_{\text{phot}}^{\text{Cit}}$, the rate constant for the Cit degradation after total depletion of Cr(VI), show a strong dependence with [Cr(VI)]₀ and with the type of photocatalyst, as can be observed in Figs. 2(a) and 2(b). The monotonous decrease of k_1 and $k_{\text{phot}}^{\text{Cit}}$ with the increasing initial Cr(VI) concentration indicates that the Cr(VI) decay with both photocatalysts is not actually a first order process, and that a progressive inhibition process takes place, attributable to Cr(III) deposition, which acts as a recombination centre.²⁴⁻³⁰ The values of k_1 and $k_{\text{phot}}^{\text{Cit}}$ (Tables S1-S4) also confirm the higher activity of UV100 compared with P25.

Although a rather significant homogeneous photochemical reaction between Cr(VI) and Cit has been reported,^{18,19} only a 40% Cr(VI) removal and less than 10% Cit degradation were observed after irradiating for 60 min a mixture of 0.8 mM Cr(VI) and 2.5 mM Cit in the absence of TiO₂ at pH 2 (Fig. S2); the value of k_1 obtained under these conditions was 10 and nearly 30 times lower than those obtained in the presence of P25 (Table S1) or UV100 (Table S2), respectively. Thus, the influence of the homogeneous reaction pathway was neglected in the analysis. Noticeably, neither OGA nor other Cit degradation product was detected after the photochemical reaction, suggesting a different reaction mechanism. The study of the homogeneous photocatalytic removal of Cr(VI) with Cit is not under the scope of this paper and will be further studied in our group.

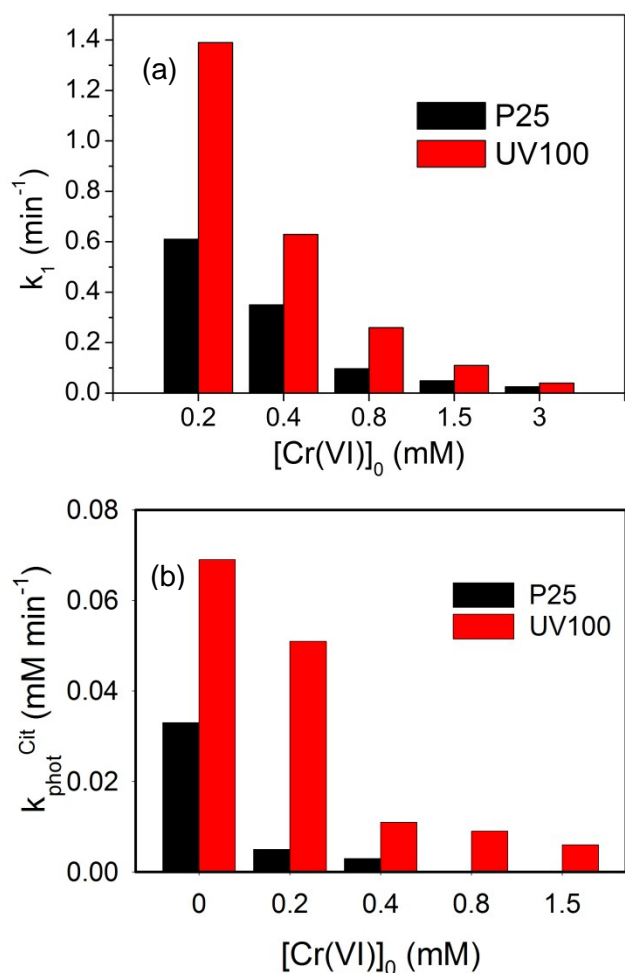


Fig. 2. Variation of (a) the pseudo-first order rate constant for Cr(VI) decay and Cit degradation up to complete Cr(VI) (k_1), and (b) the rate constant for Cit degradation after complete Cr(VI) removal (k_{phot}) with $[Cr(VI)]_0$.

Characterization of the solids after Cr(VI) removal

Fig. 3 shows the absorption spectra (expressed as absorption factor $f(\lambda)$)³¹ of the solids obtained after HP removal of Cr(VI) at $[Cr(VI)]_0 = 0.2, 0.8$ and 1.5 mM over P25 and UV100. The presence of Cr(III) on the TiO₂ surface after the Cr(VI) treatment is confirmed by the appearance of three peaks at around $\lambda = 390, 440$ and 622 nm corresponding to ${}^4A_{2g} \rightarrow {}^4T_{1g}$ (t_2^2e), ${}^4A_{2g} \rightarrow {}^4T_{1g}$ (t_2^2e) and ${}^4A_{2g} \rightarrow {}^4T_{2g}$ (t_2e^2) transitions in an octahedral field, respectively.³⁰ Also a charge-transfer absorption band at $\lambda = 450$ nm has been mentioned in Ref.³⁰, which may overlap with the ${}^4A_{2g} \rightarrow {}^4T_{1g}$ transition. For both photocatalysts, the intensity of the peaks increases with increasing $[Cr(VI)]_0$.

The solids were also analysed by TRMC (Fig. S4), a powerful tool to evaluate the lifetimes of charge carriers created in TiO₂.^{32,33} The fundamentals of this technique are summarised in the ESI. The maximum value of the TRMC signal (I_{max}) indicates the number of excess charge carriers created by the UV pulse, including decay processes during the excitation by the laser (10 ns). The decay ($I(t)$) is attributed to the decrease of the excess electrons, either by recombination or by trapping processes. Concerning the decay, i.e. the lifetime of charge carriers, a short and a long time range are usually analysed.^{20,25}

The short range decay was fixed at 40 ns after the beginning of the pulse, when decay processes during the pulse are no longer active;³³ it is represented by the I_{40ns}/I_{max} parameter, a high value indicating a low recombination speed. The long-time range was not analysed here, as it did not provide additional conclusions.

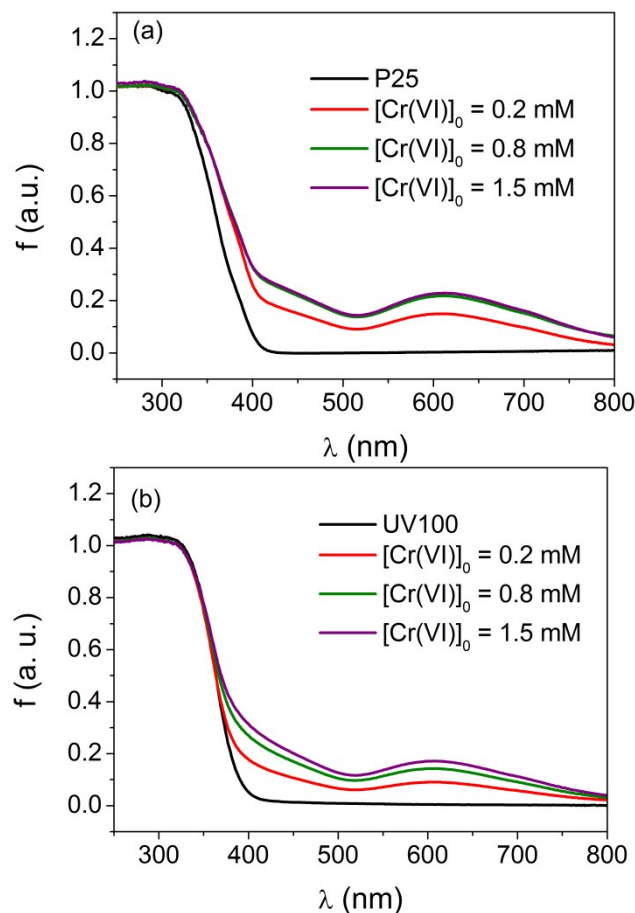


Fig. 3. Absorption spectra for the solids obtained after Cr(VI) complete removal in HP runs with $[Cr(VI)]_0 = 0.2, 0.8$ and 1.5 mM and Cit (MR = 2.5) at pH 2 over (a) P25 and (b) UV100.

Table 1 presents the parameters extracted from the TRMC analysis of the solids after complete Cr(VI) removal, the surface concentration of Cr(III) on TiO₂ obtained from TXRF measurements ($[Cr@TiO_2]$), and the Cr(III) retention efficiency (RE) calculated as:

$$RE = \frac{[Cr@TiO_2] \times [TiO_2] \times 100}{[Cr(VI)]_0} \quad (5)$$

The time for complete removal of Cr(VI) for samples used in TRMC measurements (t) is indicated also in Table 1. For $[Cr(VI)]_0 = 3$ mM (both catalysts), there was still a measurable amount of Cr(VI) after 150 min; then, these samples were not used for TRMC analysis. In general, and as obtained before in the Cr(VI)/EDTA system,^{20,25} the presence of Cr(III) on the photocatalyst lowers the I_{max} value in a small and random way. This behavior is clearer in the case of UV100, where the values of I_{max} for the solids after the Cr(VI) experiments are quite similar but clearly lower than the value for the pure material.

However, even when I_{\max} gives valuable information, the analysis of the decay, i.e. the lifetime of charge carriers, is a more robust tool that reduces the impact of experimental variations. It is seen that, for both photocatalysts, the $I_{40\text{ns}}/I_{\max}$ values decrease with the increasing incorporation of Cr(III) on the surface. The effect of Cr(III) on the surface is in good agreement with the behaviour of each photocatalyst in batch experiments: a higher amount of retained Cr(III) implies faster recombination processes, which leads to a lower removal efficiency. This agrees with the previous TRMC results.^{20,25} On the other hand, $I_{40\text{ns}}/I_{\max}$ values for P25 are, in all cases, higher than those for UV100, reflecting faster recombination processes in this last photocatalyst. This can be attributed to the lower UV100 crystalline domain, and to a higher defect concentration.²⁰ Additionally, UV100 retains higher amounts of Cr(III) than P25 but registers a lower decrease in $I_{40\text{ns}}/I_{\max}$. As UV100 has a larger area than P25 (SSA is $54.7 \text{ m}^2 \text{ g}^{-1}$ for P25 and $300 \text{ m}^2 \text{ g}^{-1}$ for UV100),²⁰ this indicates that, from all the differences between both semiconductors, P25 and UV100, the SSA seems to be the key factor to understand their different performance in the photocatalytic Cr(VI) removal in the presence of Cit.

Table 1 Parameters obtained from the TRMC measurements, time for complete Cr(VI) removal (t , min), amount of Cr on TiO_2 and percentage of Cr(III) on the surface with respect to $[\text{Cr(VI)}]_0$ of bare P25 and UV100 samples ($[\text{Cr(VI)}]_0 = 0$), and of the solids obtained after complete Cr(VI) HP disappearance.

TiO_2	$[\text{Cr(VI)}]_0$ (mM)	I_{\max} (mV)	$I_{40\text{ns}}/I_{\max}$	t (min)	$[\text{Cr@TiO}_2]$ (mmol g^{-1})	RE (%)
P25	0	85	0.50	---	---	---
	0.2	103	0.34	30	0.11	56
	0.8	87	0.31	120	0.21	26
	1.5	69	0.27	150	0.27	18
UV100	0	82	0.33	---	---	---
	0.2	43	0.28	15	0.16	78
	0.8	55	0.25	30	0.45	56
	1.5	42	0.23	45	0.67	45

It is well known that high concentrations of metals such as Cr(III) in the structure of TiO_2 lead to a lower photocatalytic activity, with an exponential increase of the recombination rate constant, k_{recomb} , through tunnelling with a decrease in the distance between metal heteroatoms, i.e., the concentration in the solid.³⁴ Therefore, it is expected that the relative decrease of the lifetime of charge carriers for each solid decreases exponentially with the concentration of Cr(III). Fig. 4 shows the lifetime of charge carriers of the solid after removal of Cr(VI) at i initial concentration with respect to pure TiO_2 ($\{I_{40\text{ns}}/I_{\max}\}_i/\{I_{40\text{ns}}/I_{\max}\}_0$) against the Cr concentration over P25 and UV100. As can be seen, a good exponential correlation ($R^2 > 0.98$) was obtained independently of the type of photocatalyst. Interestingly, when describing the concentration of retained Cr(III) with respect to the mass of TiO_2 , Cr@TiO_2 , (inset in Fig. 4), UV100 shows to be more resistant than P25 to the detrimental effect of Cr(III).

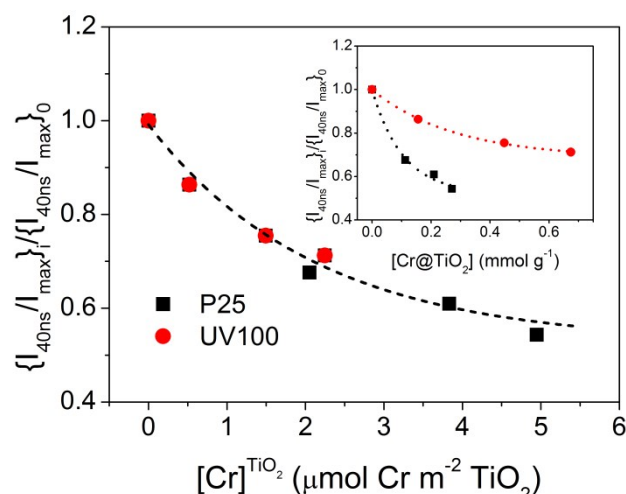


Fig. 4. $\{I_{40\text{ns}}/I_{\max}\}_i/\{I_{40\text{ns}}/I_{\max}\}_0$ vs. surface concentration of Cr ($[\text{Cr}]^{\text{TiO}_2}$) for P25 and UV100 for the solids obtained after the HP experiments with complete Cr(VI) removal ($[\text{Cr(VI)}]_0 = 0, 0.2, 0.8$ and 1.5 mM , Cit_0 (MR = 2.5), pH 2). The surface area of each photocatalyst was reported in Ref.²⁰ Inset: $\{I_{40\text{ns}}/I_{\max}\}_i/\{I_{40\text{ns}}/I_{\max}\}_0$ vs. $[\text{Cr@TiO}_2]$ for the same solids.

Effect of the electron donor

As said in the Introduction, the use of organic electron donors is a well-known strategy to increase the efficiency of HP removal of Cr(VI), given their ability to increase the lifetime of charge carriers and to the formation of highly reducing agents as Cit^\bullet . However, according to the results in this work and the previous one with EDTA,²⁵ the formation of soluble complexes of the electron donor with Cr(III) is another advantage that needs to be taken into account as it allows partial dissolution of the Cr(III) deposited on the surface during the photocatalytic reaction, preventing thus the poisoning of the photocatalyst. As mentioned before, the low selectivity towards OGA formation and the lower RE (Table 1) with increasing $[\text{Cr(VI)}]_0$ can be explained by the formation of soluble complexes between Cr(III) and Cit^{35-37} or with other degradation by-products. In fact, as shown in Fig. 5, the comparison of the TRMC profiles for EDTA and Cit (2 mM, absence of Cr(VI)) adsorbed on P25 (1 g L^{-1}) at pH 2 reveals that the lifetime of charge carriers is larger for the systems with Cit, indicating that Cit is a better electron donor. However, after complete Cr(VI) removal, P25 and UV100 retained 0.27 and 0.45 mmol g^{-1} of Cr(III), respectively, in the presence of Cit (Table 1), and 0.05 and 0.11 mmol g^{-1} of Cr(III) in the presence of EDTA.²⁵ This is directly related with the higher complexation constant of Cr(III)-EDTA compared with that for Cr(III)-Cit ($\text{Log}K_{\text{ML}}^{\text{EDTA}} = 23.4$ y $\text{Log}K_{\text{ML}}^{\text{Cit}} = 8.7$).³⁷

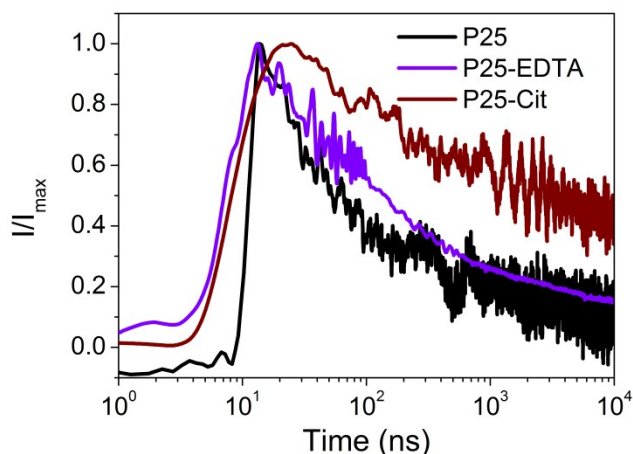


Fig. 5. TRMC temporal profiles for P25 and P25 after adsorption of Cit and EDTA. Conditions: [P25] = 1 g L⁻¹, [EDTA] or [Cit] = 2 mM, pH 2.

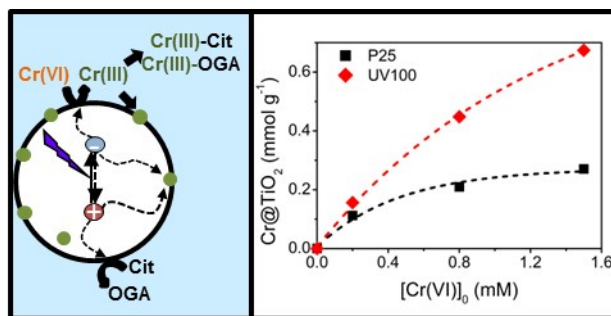
Conclusions

In the Cr(VI) HP reduction in the presence of Cit, a concerted reaction with Cit degradation occurs, regardless of the type of TiO₂ and the initial concentration of the chemical species. For both evaluated photocatalysts, P25 and UV100, the pseudo-first order rate constant was lower with increasing [Cr(VI)]₀, and the same behaviour was observed for the degradation of Cit after Cr(VI) complete removal. Both effects were demonstrated to be associated to a recombination rate enhanced by the retention of Cr(III) on the surface of TiO₂. Cr(III) can act as a recombination centre and its detrimental effect is more intense in P25 because of its lower surface area compared with that of UV100.

The nature of the sacrificial agent not only influences the rate and efficiency of the photocatalytic Cr(VI) removal, but also the stability of the photocatalyst by preventing Cr(III) deposition. This work confirms our previous statement²⁵ that the effect of a synergistic agent able to form soluble complexes with Cr(III) can be extended as a general behaviour of reducing oligocarboxylic acids in photocatalytic systems.

Notes and references

- J.A. Izbicki, T.D. Bullen, P. Martin, B. Schroth, *Appl. Geochem.*, 2012, **27**, 841.
- R. Dai, J. Liu, C. Yu, J. Liu, Y. Lan, B. Deng, *Environ. Sci. Technol.*, 2010, **44**, 6959.
- M. Owlad, M.K. Aroua, W.A.W. Daud, S. Baroutian, *Water Air Soil Pollut.*, 2009, **200**, 59.
- WHO, *Guidelines for drinking-water quality*, 4th ed., World Health Organization, Geneva, 2011, p. 340. Available at: http://whqlibdoc.who.int/publications/2011/9789241548151_eng.pdf (last accessed: 10 August 2013).
- Kooragang Island Orica chemical leak. Available at: [http://www.parliament.nsw.gov.au/prod/parlment/committee.nsf/0/2aaffe5684a88ac6ca2579ac007c4430/\\$FILE/120223%20Orica%20Report.pdf](http://www.parliament.nsw.gov.au/prod/parlment/committee.nsf/0/2aaffe5684a88ac6ca2579ac007c4430/$FILE/120223%20Orica%20Report.pdf) (last accessed: 7 November 2015).
- C. Vasilatos, I. Megremi, M. Economou-Eliopoulos, I. Mitsis, *Hellenic J. Geosci.*, 2008, **43**, 57.
- C.E. Barrera-Díaz, V. Lugo-Lugo, B. Bilyeu, *J. Hazard. Mater.*, 2012, **223–224**, 1.
- M.I. Litter, *Appl. Catal. B: Environ.*, 1999, **23**, 89.
- M.I. Litter, *Adv. Chem. Eng.*, 2009, **36**, 37.
- M.I. Litter, N. Quici, in: B.I. Kharisov, O.V. Kharissova, H.V. Rasika Dias (Eds.), *Nanomaterials for Environmental Protection*, John Wiley & Sons, Hoboken (NJ) Chap. 9, pp. 143-167, Published Online: 9 August 2014, DOI: 10.1002/9781118845530.
- M.I. Litter, *Pure Appl. Chem.* 2015, **87**, 557.
- M.R. Prairie, L.R. Evans, B.M. Stange, S.L. Martinez, *Environ. Sci. Technol.*, 1993, **27**, 1776.
- L. Wang, N. Wang, L. Zhu, H. Yu, H. Tang, *J. Hazard. Mater.*, 2008, **152**, 93.
- J.J. Testa, M.A. Grela, M.I. Litter, *Langmuir*, 2001, **17**, 3515.
- J.J. Testa, M.A. Grela, M.I. Litter, *Environ. Sci. Technol.*, 2004, **38**, 1589.
- J.M. Meichtry, M. Brusa, G. Mailhot, M.A. Grela, M.I. Litter, *Appl. Catal. B: Environ.*, 2007, **71**, 101.
- J. M. Meichtry, Doctoral Thesis, University of Buenos Aires, 2011.
- L. Yang, Y. Xiao, S. Liu, Y. Li, Q. Cai, S. Luo, G. Zeng, *Appl. Catal. B: Environ.*, 2010, **94**, 142. Z. Xu, S. Bai, J. Liang, L. Zhou, Y. Lan, *Mater. Sci. Eng. C*, 2013, **33**, 2192.
- J.M. Meichtry, C. Colbeau-Justin, G. Custo, M.I. Litter, *Appl. Catal. B: Environ.*, 2014, **144**, 189.
- U. Siemon, D. Bahnemann, J.J. Testa, D. Rodríguez, N. Bruno, M.I. Litter, *J. Photochem. Photobiol. A*, 2002, **148**, 247.
- ASTM Standards D 1687, 1999.
- J.M. Meichtry, N. Quici, G. Mailhot, M.I. Litter, *Appl. Catal. B*, 2011, **102**, 454.
- J.M. Meichtry, N. Quici, G. Mailhot, M.I. Litter, *Appl. Catal. B*, 2011, **102**, 555.
- J.M. Meichtry, C. Colbeau-Justin, G. Custo, M.I. Litter, *Catal. Today*, 2014, **224**, 236.
- Y. Ku, I.-L. Jung, *Water Res.*, 2011, **35**, 135.
- N. Wang, Y. Xu, L. Zhu, X. Shen, H. Tang, *J. Photochem. Photobiol. A*, 2009, **201**, 121.
- S. Tuprakay, W. Liengcharernsit, *J. Hazard. Mater.*, 2005, **124**, 53.
- H. Kyung, J. Lee, W. Choi, *Environ. Sci. Technol.*, 2005, **39**, 2376.
- S.Ould-Chikh, O. Proux, P. Afanasiev, L. Khrouz, M.N. Hedhili, D.H. Anjum, M. Harb, C. Geantet, J.-M. Basset, E. Puzenat, *Chem. Sus. Chem.*, 2014, **7**, 1361.
- S.E. Braslavsky, *Pure Appl. Chem.*, 2007, **79**, 293
- C. Colbeau-Justin, M. Kunst, D. Huguénin, *J. Mater. Sci.*, 2003, **38**, 2429.
- M. Kunst, F. Goubard, C. Colbeau-Justin, F. Wünsch, *Mater. Sci. Eng. C*, 2007, **27**, 19.
- J. Z. Bloh, R. Dillert and D. W. Bahnemann, *ChemCatChem*, 2013, **5**, 774–778.
- C. Gabriel, C.P. Raptopoulou, A. Terzis, V. Tangoulis, C. Mateescu, A. Salifoglou, *Inorg. Chem.*, 2007, **46**, 2998.
- C. Gabriel, C.P. Raptopoulou, C. Drouza, N. Lalioti, A. Salifoglou, *Polyhedron*, 2009, **28**, 3209.
- L. Jean-Soro, F. Bordas, J.-C. Bollinger, *Environ. Pollut.*, 2012, **164**, 175.



A larger specific area makes UV100 more efficient than P25 for Cr(VI) and citric acid removal. Citric and 3-oxoglutaric acids prevent surface deposition of Cr(III) recombining centers.